Neuron
Article

Burst-Timing-Dependent Plasticity of NMDA Receptor-Mediated Transmission in Midbrain Dopamine Neurons

Mark T. Harnett,[1,2,3] Brian E. Bernier,[1,2,3] Kee-Chan Ahn,[1,2,3] and Hitoshi Morikawa[1,2,3,*]
[1]Institute for Neuroscience
[2]Waggoner Center for Alcohol and Addiction Research
[3]Section of Neurobiology
University of Texas at Austin, Austin, TX 78712, USA
*Correspondence: morikawa@mail.utexas.edu
DOI 10.1016/j.neuron.2009.05.011

SUMMARY

Bursts of spikes triggered by sensory stimuli in midbrain dopamine neurons evoke phasic release of dopamine in target brain areas, driving reward-based reinforcement learning and goal-directed behavior. NMDA-type glutamate receptors (NMDARs) play a critical role in the generation of these bursts. Here we report LTP of NMDAR-mediated excitatory transmission onto dopamine neurons in the substantia nigra. Induction of LTP requires burst-evoked Ca^{2+} signals amplified by preceding metabotropic neurotransmitter inputs in addition to the activation of NMDARs themselves. PKA activity gates LTP induction by regulating the magnitude of Ca^{2+} signal amplification. This form of plasticity is associative, input specific, reversible, and depends on the relative timing of synaptic input and postsynaptic bursting in a manner analogous to the timing rule for cue-reward learning paradigms in behaving animals. NMDAR plasticity might thus represent a potential neural substrate for conditioned dopamine neuron burst responses to environmental stimuli acquired during reward-based learning.

INTRODUCTION

The appropriate association between environmental cues and motivational valence is crucial for the brain to accurately guide behavior. Dopamine (DA) neurons, located in the substantia nigra pars compacta (SNc) and ventral tegmental area (VTA), are thought to assign positive values to objects and experiences in order to effectively influence decision-making strategies (Montague et al., 2004). In vivo experiments in non-human primates and rodents coupled with human functional imaging and computational modeling studies have suggested that this occurs through changes in DA neuron firing rate, which encode reward prediction errors (D'Ardenne et al., 2008; Montague et al., 1996; Pan et al., 2005; Schultz, 1998). As such, DA neurons transition from tonic single-spike firing (1–5 Hz) to burst firing (two to ten spikes at 10–50 Hz) in response to the unexpected presentation of primary rewards. Intriguingly, the burst response shifts in time to reward-predicting cues after conditioning with repeated cue-reward pairing. However, the locus of neural plasticity responsible for this conditioned DA neuron response remains elusive.

Glutamatergic inputs activating NMDA receptors (NMDARs) have been shown to drive the transition from slow, tonic firing to burst firing in DA neurons (Chergui et al., 1994; Morikawa et al., 2003; Overton and Clark, 1997; Tong et al., 1996; Zweifel et al., 2009), although AMPA receptors (AMPARs) might also play a role (Blythe et al., 2007). Therefore, potentiation of NMDAR-dependent excitation of DA neurons might contribute to the development of the conditioned burst response. Despite numerous studies describing the plasticity of AMPARs in DA neurons (Jones and Bonci, 2005; Kauer and Malenka, 2007), synaptic activity-dependent plasticity of NMDAR-mediated transmission has yet to be demonstrated (but see Borgland et al. [2006], Schilstrom et al. [2006], and Ungless et al. [2003] for enhancement of NMDAR function caused by metabotropic receptor agonists).

Ca^{2+} signaling, triggered by either postsynaptic action potentials (APs) or local synaptic events, is implicated in the plasticity of synapses throughout the CNS (Linden, 1999; Sjostrom and Nelson, 2002). We have previously shown that AP-evoked Ca^{2+} signals can be amplified by the activation of metabotropic glutamate receptors (mGluRs) and other neurotransmitter receptors coupled to phosphoinositide (PI) hydrolysis in DA neurons (Cui et al., 2007). This amplification results from an elevation in cytosolic inositol trisphosphate (IP_3) levels, leading to enhanced Ca^{2+}-induced Ca^{2+} release (CICR) through IP_3 receptors (IP_3Rs) located on intracellular Ca^{2+} stores. IP_3, generated by activation of PI-coupled neurotransmitter receptors, and Ca^{2+}, provided by AP-induced influx, thus synergistically coactivate IP_3Rs (Taylor and Laude, 2002). In this study, we asked if this synergistic Ca^{2+} signaling could drive plasticity of NMDAR-mediated transmission onto DA neurons. We found that repeated pairing of sustained synaptic stimulation with burst firing results in long-term potentiation (LTP) of NMDAR excitatory postsynaptic currents (EPSCs). The induction of LTP requires PI-coupled receptor-mediated facilitation of burst-induced Ca^{2+} signals and NMDAR activation. LTP induction is also gated by protein kinase A (PKA),

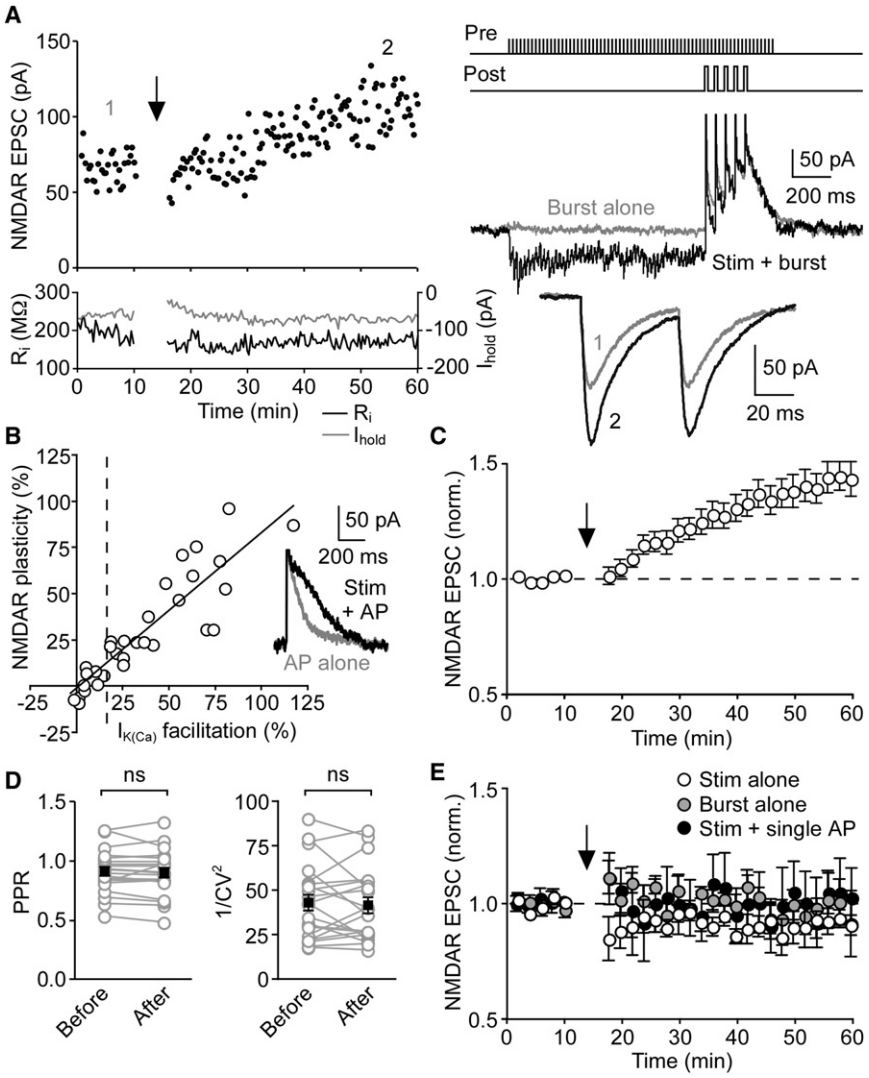

Figure 1. Repeated Synaptic Stimulation-Burst Pairing Induces LTP of NMDAR EPSCs in DA Neurons

(A) Representative experiment showing LTP of NMDAR EPSCs. Left: Time graph of NMDAR EPSC amplitude, input resistance (R_i, black), and holding current (I_{hold}, gray). The LTP induction protocol, which consisted of ten synaptic stimulation-burst pairings (illustrated at top right), was delivered at the time indicated by the arrow. Middle right: Current traces evoked by burst alone (gray) and synaptic stimulation-burst pairing (black). Bottom right: Traces of EPSCs (averaged over 10 min) at times indicated by numbers in the EPSC time graph.

(B) Relationship between the magnitude of NMDAR LTP and facilitation of AP-evoked $I_{K(Ca)}$ by preceding synaptic stimulation for 31 neurons. Solid line is a linear fit to the data. Dashed vertical line indicates 15% $I_{K(Ca)}$ facilitation. Inset at right shows traces of $I_{K(Ca)}$ for a single AP alone (gray) and an AP following synaptic stimulation (black) from the same neuron as in (A).

(C) Summary time graph of NMDAR LTP for neurons that exhibited >15% $I_{K(Ca)}$ facilitation (n = 21). Each symbol represents mean normalized EPSC amplitude from a 2 min window.

(D) PPR (left) and $1/CV^2$ (right) were not significantly altered after LTP induction for the 21 neurons in (C). Black squares indicate mean.

(E) Summary time graph showing that synaptic stimulation alone (n = 6), burst alone (n = 6), and pairing synaptic stimulation with a single AP (n = 5) all failed to induce NMDAR LTP. Note that a small LTD was induced with synaptic stimulation alone. Error bars indicate standard error of the mean (SEM).

which regulates IP_3R sensitivity. We further show that NMDAR LTP is input specific, requires appropriately timed presynaptic and postsynaptic activity, and can be reversed by repetitive presynaptic stimulation without postsynaptic firing.

RESULTS

Activity-Dependent LTP of NMDAR EPSCs in DA Neurons

Whole-cell voltage-clamp recordings were made from DA neurons in the SNc (~90%) and VTA (~10%) using rat midbrain slices. Previous studies examining the conditioning of DA neuron responses in behaving animals, in which larger number of neurons were sampled from the SNc than the VTA, have reported similar response profiles in these two areas (Mirenowicz and Schultz, 1996; Pan et al., 2005; Schultz, 1998). A bipolar stimulating electrode was placed 50–150 μm rostral to the recorded neuron. Pharmacologically isolated NMDAR EPSCs were recorded at −62 mV in low Mg^{2+} (0.1 mM) to remove blockade of NMDARs. After 10 min of baseline EPSC recording, we delivered an LTP induction protocol consisting of a train of presynaptic stimulation (70 stimuli at 50 Hz) paired with a burst of five postsynaptic unclamped APs at 20 Hz, which mimics burst firing observed in behaving rats (Hyland et al., 2002). The onset of the burst was delayed by 1 s from that of the synaptic stimulation train. We found that repetitive synaptic stimulation-burst pairing (ten times every 20 s) resulted in LTP of NMDAR EPSCs in some but not all neurons tested (Figure 1A). The pattern of synaptic stimulation used in the induction protocol can augment AP-induced Ca^{2+} signals via activation of PI-coupled receptors, mainly $mGluR_1$ (Cui et al., 2007). To address the role of AP-evoked Ca^{2+} signals in LTP induction, we measured small-conductance Ca^{2+}-sensitive K^+ (SK) currents ($I_{K(Ca)}$) activated by unclamped APs (see Experimental Procedures). Immediately before induction, we tested each neuron for facilitation of $I_{K(Ca)}$ following synaptic stimulation by evoking a single AP at 60 ms after the offset of a 1 s stimulation train (example traces shown in inset of Figure 1B). The magnitude of NMDAR LTP, determined 30–40 min after the induction, was positively correlated with that of $I_{K(Ca)}$ facilitation (n = 31, r^2 = 0.80) (Figure 1B). However,

NMDAR LTP was not correlated with the size of $I_{K(Ca)}$ itself or with baseline EPSC amplitude (see Figure S1 available online). On average, NMDAR EPSCs were potentiated by 43% ± 6% in 21 neurons that exhibited $I_{K(Ca)}$ facilitation >15%, whereas no LTP was observed when $I_{K(Ca)}$ facilitation was <15% (1% ± 2% change, n = 10) (Figure 1C). The paired-pulse ratio (PPR, 50-ms interstimulus interval, expressed as $EPSC_2/EPSC_1$) and the coefficient of variation (CV, expressed as $1/CV^2$) of EPSCs were not significantly changed in 21 neurons that exhibited LTP (Figure 1D), suggesting a postsynaptic locus of LTP expression (Malinow and Tsien, 1990; Zalutsky and Nicoll, 1990). Repeated delivery of postsynaptic burst firing alone failed to induce LTP of NMDAR EPSCs (0% ± 3% change, n = 6), while synaptic stimulation alone produced a small but significant LTD (−8% ± 4% change, n = 6) (Figure 1E). Furthermore, LTP was not observed when the burst was replaced with a single AP during pairing (−1% ± 10% change, n = 5). Together, these results suggest that synaptic facilitation of burst-induced Ca^{2+} signaling is involved in the induction of NMDAR LTP. Due to the correlation between $I_{K(Ca)}$ facilitation and LTP in our initial finding, subsequent experiments were conducted in neurons that exhibited >15% $I_{K(Ca)}$ facilitation unless otherwise stated (see Table S1).

To confirm that this form of plasticity could be induced in physiological Mg^{2+}, we recorded NMDAR EPSCs in 1.2 mM Mg^{2+} at slightly depolarized holding potentials (−47 to −62 mV) using Cs^+-based internal solution to enhance the resolution of small NMDAR EPSCs (23 ± 3 pA, n = 8). Measurable $I_{K(Ca)}$ was not observed in these experiments, most likely due to the low permeability of SK channels to Cs^+ (Shin et al., 2005). Pairing presynaptic stimulation with postsynaptic bursting produced LTP >10% in six of eight neurons tested in physiological Mg^{2+} (23% ± 4% change, n = 6) (Figure S2).

We also examined the effect of the burst pairing protocol on AMPAR-mediated transmission. Here, AMPAR EPSCs were recorded at −62 or −77 mV in 1.2 mM Mg^{2+} with NMDARs intact, whereas synaptic stimulation-burst pairing was delivered at −62 mV. This resulted in LTD of EPSCs (−29% ± 3% change, n = 5) (Figure S3). The magnitude of LTD showed no correlation with $I_{K(Ca)}$ facilitation by synaptic stimulation (r^2 = 0.0003) (Figure S3C). Furthermore, there was no difference ($p > 0.5$) in the amount of LTD expressed when postsynaptic burst firing was omitted and neurons received the synaptic stimulation train alone (−26% ± 3% change, n = 3) (Figures S3B and S3C). It should be noted that the intracellular machinery responsible for the induction of AMPAR LTP might be "washed-out" during whole-cell recordings in DA neurons (Bonci and Malenka, 1999).

Induction of NMDAR LTP Requires PI-Coupled Receptor Activation and Release of Ca^{2+} from Internal Stores

Activation of PI-coupled receptors facilitates AP-evoked Ca^{2+} signals in DA neurons via an increase in IP_3 levels, which enhances IP_3R-dependent CICR from intracellular stores (Cui et al., 2007). We thus examined the role of this Ca^{2+} signaling cascade in NMDAR LTP. Treatment of slices with cyclopiazonic acid (CPA, 10 μM), which depletes intracellular Ca^{2+} stores (Seidler et al., 1989), eliminated the facilitation of $I_{K(Ca)}$ by synaptic stimulation (0% ± 2%, n = 6) as well as the induction of NMDAR LTP (2% ± 4% change, n = 6) (Figure 2). Pharmacological blockade of $mGluR_1$ together with muscarinic acetylcholine and α_1-adrenergic receptors, other major PI-coupled neurotransmitter receptors expressed in DA neurons (Fiorillo and Williams, 2000; Paladini and Williams, 2004), also abolished $I_{K(Ca)}$ facilitation (2% ± 3%, n = 6) and NMDAR LTP (−6% ± 4% change, n = 6) (Figures 2B and 2C). We further confirmed that intracellular BAPTA (100 μM) blocked $I_{K(Ca)}$ facilitation (4% ± 1%, n = 6) and NMDAR LTP (−1% ± 5% change, n = 6). Together with the data presented in Figures 1B and 1E, these results demonstrate that Ca^{2+} store-dependent enhancement of burst-induced Ca^{2+} signals is critical for LTP induction.

PKA Regulates PI-Coupled Receptor-Mediated Facilitation of Ca^{2+} Signals and Induction of NMDAR LTP

IP_3 sensitivity of IP_3Rs can be increased by PKA-mediated phosphorylation (Tang et al., 2003; Wagner et al., 2008). To examine the role of PKA, we loaded recorded neurons with the specific PKA inhibitor PKI (100–200 μM) through the whole-cell pipette. We first tested the effect of PKI on IP_3 sensitivity of IP_3Rs by performing flash photolysis of caged IP_3 using different ultraviolet irradiation (UV) pulse intensities (expressed in μF; see Experimental Procedures) to vary the concentration of IP_3 released and measured the resulting SK-mediated outward current (I_{IP3}) (Figure 3A). Intracellular PKI significantly increased the UV pulse intensity producing half maximal I_{IP3} amplitude (138 ± 12 μF in control, n = 5 versus 220 ± 37 μF in PKI, n = 7, $p < 0.05$) (Figure 3B), suggesting that IP_3 sensitivity is enhanced by tonic PKA activity. Although PKA is not known to modulate SK channel function, recent evidence indicates that PKA phosphorylation can regulate surface expression of SK2 channels (Lin et al., 2008; Ren et al., 2006). However, PKI failed to alter the maximal I_{IP3} amplitude (data not shown). This might be due to the predominant expression of SK3 channels in DA neurons (Wolfart et al., 2001).

PKI also significantly reduced the magnitude of $I_{K(Ca)}$ facilitation caused by bath perfusion of the mGluR agonist DHPG (1 μM) (92% ± 21% in control, n = 13 versus 27% ± 10% in PKI, n = 10, $p < 0.01$) (Figures 3C and 3D). In five PKI-loaded neurons that exhibited <20% $I_{K(Ca)}$ facilitation (9% ± 3%) in response to 1 μM DHPG, higher concentrations of DHPG (5–10 μM), which should further elevate cytosolic IP_3 levels, produced significantly larger $I_{K(Ca)}$ facilitation (221% ± 51%, $p < 0.05$) (Figure 3E), consistent with the idea that PKI reduced the IP_3 sensitivity of IP_3Rs.

We next tested the effect of PKI on NMDAR LTP. Intracellular PKI suppressed $I_{K(Ca)}$ facilitation by synaptic stimulation (9% ± 3%, n = 7) as well as the induction of LTP (−3% ± 6% change, n = 7) (Figures 3F and 3G). In contrast, intracellular dialysis with the PKC inhibitor chelerythrine (10 μM), which has been shown to block NMDAR LTP in the hippocampus (Kwon and Castillo, 2008), had no significant effect on $I_{K(Ca)}$ facilitation or NMDAR LTP (Figures 3D, 3F, and 3G). Together, these data demonstrate that PKA activity regulates the induction of NMDAR LTP by augmenting PI-coupled receptor-mediated facilitation of Ca^{2+} signals.

NMDAR LTP Is DA Independent

DA neuron bursts are thought to provide a plasticity signal in projection areas via phasic DA release, thus driving

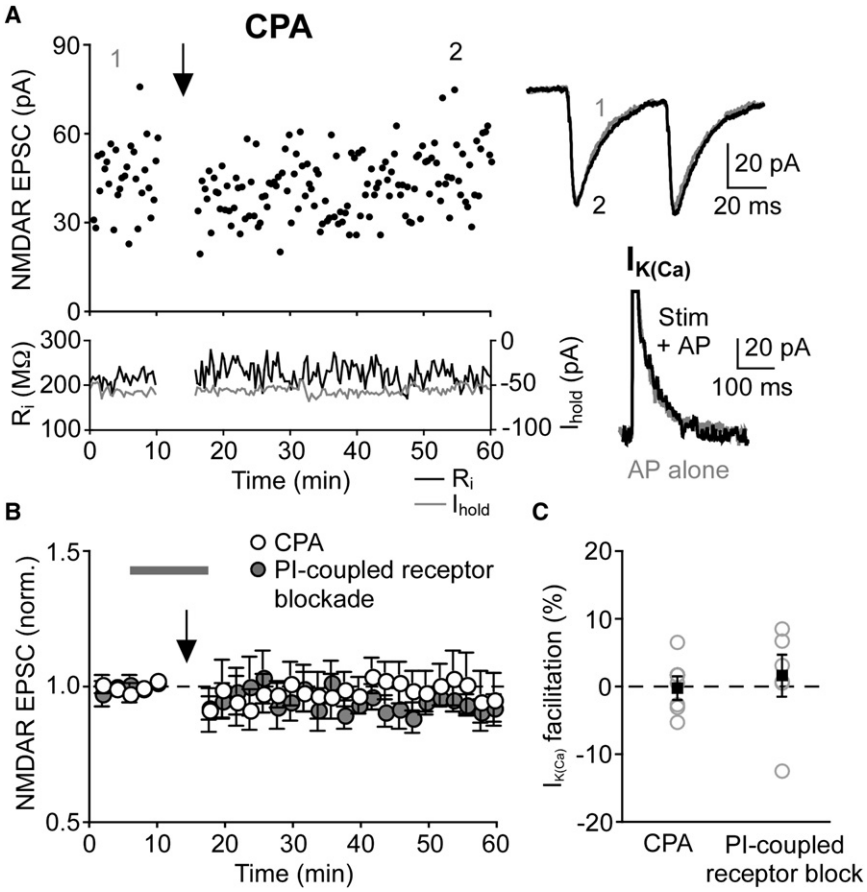

Figure 2. PI-Coupled Receptor Activation and Release of Ca^{2+} from Internal Stores Is Necessary for NMDAR LTP Induction

(A) Time graph of a representative experiment conducted in the presence of CPA (10 μM). Sample traces to the right show average NMDAR EPSCs before (1) and after (2) synaptic stimulation-burst pairing (top traces) and $I_{K(Ca)}$ with (black) and without (gray) synaptic stimulation (bottom traces). Note the lack of facilitation of $I_{K(Ca)}$ by synaptic stimulation.

(B) Summary time graph of experiments conducted in the presence of CPA (n = 6) and experiments where PI-coupled receptors were blocked during the induction, as indicated by the gray bar, with a cocktail containing the $mGluR_1$ antagonist CPCCOEt (50–75 μM), the muscarinic acetylcholine receptor antagonist scopolamine (100 nM), and the α_1-adrenergic receptor antagonist prazosin (1 μM) (n = 6).

(C) Summary graph depicting lack of significant facilitation of $I_{K(Ca)}$ by synaptic stimulation in CPA or during PI-coupled receptor blockade. Gray open circles indicate individual experiments; black squares represent mean. Error bars indicate SEM.

reward-based learning (Schultz, 1998). DA neuron bursts might also trigger Ca^{2+}-dependent dendritic release of DA in the SNc (Beckstead et al., 2004; Chen and Rice, 2001). Furthermore, activation of DA $D_{1/5}$ receptors can produce potentiation of NMDAR EPSCs (Schilstrom et al., 2006), raising the possibility that DA might play a role in LTP induction. However, significant NMDAR LTP was observed (38% ± 9% change, n = 5) even when the DA $D_{1/5}$ receptor antagonist SCH 23390 (1 μM) was present during induction (Figure S4). The DA D_2 receptor antagonist eticlopride (100–200 nM) was always present in the extracellular solution in this study to block D_2 receptor-mediated IPSCs (Beckstead et al., 2004). Thus, burst-induced DA release is not involved in the induction of NMDAR LTP in DA neurons.

NMDAR Activation Is Necessary for Induction of NMDAR LTP

Recent studies on the plasticity of NMDARs at hippocampal mossy fiber synapses indicate that activation of NMDARs, in addition to activation of mGluRs, is required during LTP induction (Kwon and Castillo, 2008; Rebola et al., 2008). In order to test this possibility in DA neurons, we acutely blocked NMDARs with the NMDAR antagonist DL-AP5 (50–100 μM) during induction (Figure 4). Perfusion of DL-AP5 after 10 min of baseline recording rapidly and completely blocked NMDAR EPSCs (from 44 ± 11 pA to 2 ± 1 pA, n = 4), and the burst pairing protocol was delivered thereafter. DL-AP5 was washed out immediately after induction. Despite robust facilitation in all neurons tested (56% ± 13%, n = 4), none exhibited LTP of NMDAR EPSCs (−1% ± 2% change) (Figure 4B). We confirmed that the washout of DL-AP5 (100 μM) was complete in ~30 min when no burst pairing protocol was delivered (n = 3). Therefore, the induction of NMDAR LTP requires the activation of NMDARs themselves.

NMDAR Plasticity Is Induced in a Burst-Timing-Dependent Manner

We next examined if LTP induction is dependent on the relative timing between synaptic stimulation and burst firing. In our routine induction protocol, there is a 1 s delay between the onset of the 1.4 s synaptic stimulation train and that of the burst. When this delay was omitted, i.e., when the onset of the burst was shifted forward to coincide with that of synaptic stimulation, no LTP was induced (−3% ± 10% change, n = 4) (Figure 5A). Similarly, no significant LTP was observed when the burst was elicited with a delay of 200 ms after the onset of synaptic stimulation (3% ± 5% change, n = 3). However, sizable LTP was induced when the burst occurred with a 500 ms delay during the pairing protocol (20% ± 6% change, n = 5), although reduced in magnitude compared with the LTP induced with a 1 s burst delay. In line with these observations, we found that the magnitude of $I_{K(Ca)}$ facilitation gradually increased during 1 s synaptic stimulation in these neurons tested for the burst-timing dependence of LTP induction (Figure 5B), most likely reflecting gradual increases in cytosolic IP_3 levels. In a separate series of experiments, we performed fluorescence imaging of burst-induced Ca^{2+} signals using fluo-5F (50 μM) as a Ca^{2+} indicator and examined the burst-timing dependence of facilitation produced by a 1.4 s

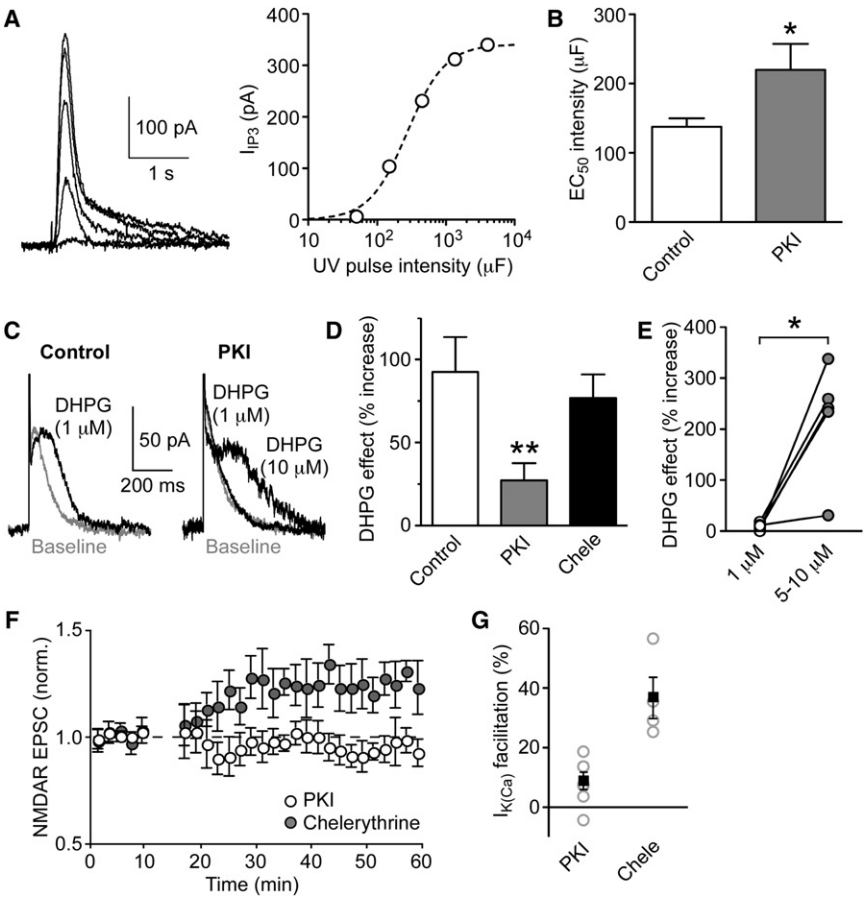

Figure 3. PKA Regulates IP_3R Sensitivity and NMDAR LTP Induction

(A) Left: Traces of I_{IP3} evoked with different UV pulse intensities in a PKI-loaded neuron. Right: I_{IP3} amplitude is plotted versus UV pulse intensity, expressed in terms of the capacitance (μF) of the flash photolysis system, in the same neuron. Dotted line represents fit to a logistic equation. EC_{50} intensity was 275 μF in this neuron.

(B) Bar graph showing that PKI (n = 7) significantly increased the EC_{50} intensity to produce I_{IP3}. *p < 0.05 versus control internal solution (n = 5).

(C) Representative traces illustrating the effects of DHPG on single AP-evoked $I_{K(Ca)}$ recorded with a control internal solution (left) or PKI (200 μM; right).

(D) Summary bar graph demonstrating that PKI (n = 10), but not chelerythrine (n = 6), significantly reduced the effect of DHPG (1 μM) on $I_{K(Ca)}$. **p < 0.01 versus control internal solution (n = 13).

(E) The effects of DHPG at 1 μM versus 5–10 μM are plotted in five PKI-loaded neurons. *p < 0.05.

(F) Summary time graph showing that PKI (n = 7), but not chelerythrine (n = 4), blocked NMDAR LTP.

(G) Summary graph showing the magnitude of $I_{K(Ca)}$ facilitation by synaptic stimulation in PKI and chelerythrine. Gray open circles indicate individual experiments; black squares represent mean. Error bars indicate SEM.

synaptic stimulation train. The magnitude of facilitation of burst-evoked fluorescence change also gradually increased as the delay between the onset of synaptic stimulation and that of the burst was prolonged up to 1 s in 6 neurons tested (Figures 5C and 5D). Synaptic stimulation increased burst-evoked fluorescence change by 35% ± 5% (n = 6) at 1 s delay. This increase was abolished by CPCCOEt (75 μM, n = 2), consistent with the role of $mGluR_1$ in synaptic facilitation (Cui et al., 2007), but was unaffected by DL-AP5 (50–100 μM, n = 4) (Figure S5). No AP5-sensitive fluorescence change was observed with synaptic stimulation alone, indicating that NMDAR-mediated Ca^{2+} influx was not detected with our imaging system.

Next, we delayed the burst until after the offset of the synaptic stimulation train. This resulted in a significant decrease in LTP with an interval of 60 ms (13% ± 14% change, n = 4) and near complete lack of LTP with a 120 ms interval (6% ± 5% change, n = 5) (Figures 5A and 5E). In the five neurons in which LTP induction was attempted with a 120 ms interval, facilitation of $I_{K(Ca)}$ at 120 ms after the offset of synaptic stimulation was indistinguishable from that at 60 ms, the interval routinely used to assess $I_{K(Ca)}$ facilitation (Figure 5B). Furthermore, in Ca^{2+} imaging experiments, facilitation of burst-evoked fluorescence change was not significantly reduced when the burst was elicited at 120 ms after the offset of the 1.4 s synaptic stimulation train (Figures 5C and 5D), indicating that the decrease in LTP is not due to a reduction in synaptic facilitation of Ca^{2+} signaling. Indeed, IP_3-mediated enhancement of Ca^{2+} signals has been shown to last for hundreds of milliseconds because of prolonged lifetime of IP_3 binding to IP_3Rs (Sarkisov and Wang, 2008). In contrast, NMDAR EPSCs evoked by synaptic stimulation decayed by 80% ± 4% at 60 ms after the offset of stimulation in the four neurons tested at 60 ms interval for LTP induction, whereas the decay of NMDAR EPSCs was almost complete (96% ± 1%) at 120 ms in the five neurons tested for 120 ms interval. This implies that the burst might need to occur while NMDARs are activated during induction. Therefore, the burst-timing dependence of LTP induction described here is consistent with the requirement of both PI-coupled receptor-mediated facilitation of burst-induced Ca^{2+} signals (Figure 2) and activation of NMDARs (Figure 4).

Finally, we evoked burst firing before the onset of synaptic stimulation during induction. Interestingly, sizable NMDAR LTD was observed when the onset of the burst was placed 250 ms before that of the synaptic stimulation train (−22% ± 7% change, n = 4) (Figure 5A). There was no significant change in either PPR or $1/CV^2$ (0.84 ± 0.07 versus 0.86 ± 0.06 and 41 ± 12 versus 39 ± 10, respectively; p > 0.5 for both parameters), suggesting a postsynaptic locus of LTD expression as for LTP. When the interval between burst onset and synaptic stimulation was increased to 500 ms, where burst-induced Ca^{2+} rise had minimal overlap, if any, with synaptic stimulation, the magnitude of LTD was reduced to a level comparable to that induced by presynaptic stimulation alone (500 ms before onset: −10% ± 4% change,

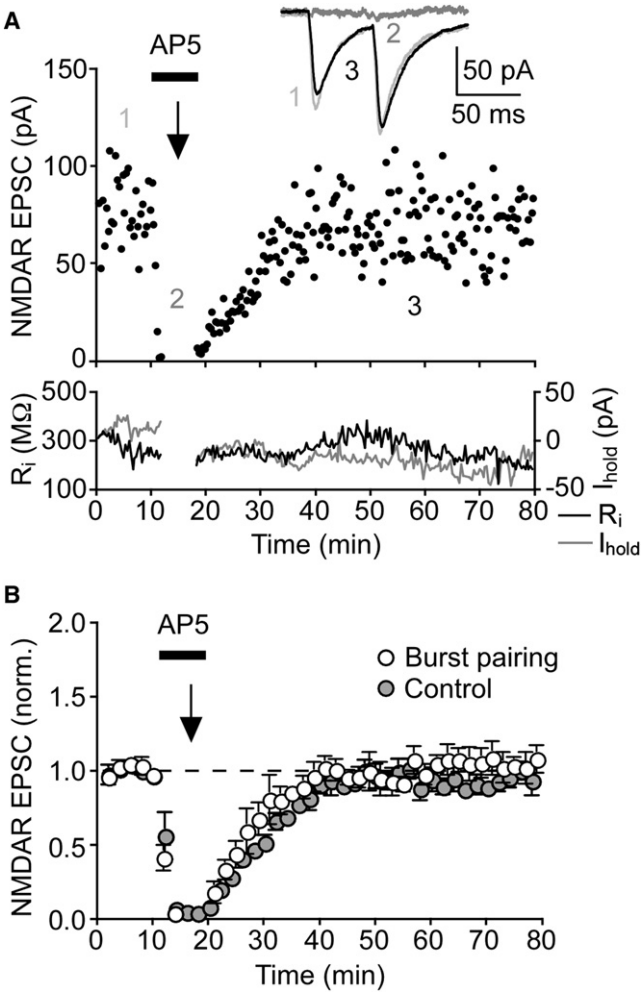

Figure 4. NMDAR LTP Requires NMDAR Activation during Synaptic Stimulation-Burst Pairing

(A) Transiently blocking NMDARs with DL-AP5 (100 μM) during delivery of the induction protocol, as indicated by the black bar, prevented the development of LTP in this example experiment. Average NMDAR EPSCs taken at the times indicated are shown in inset for control (1), in AP5 (2), and after LTP induction and AP5 washout (3).

(B) Summary time graph of experiments where LTP was blocked by DL-AP5 (50–100 μM) perfused during the induction (n = 4). Summary of control experiments is also shown, where DL-AP5 (100 μM) was perfused and washed out without delivery of the induction protocol (n = 3). Error bars indicate SEM.

n = 4 versus synaptic stimulation alone: −8% ± 4% change, n = 6, $p > 0.5$). Together, these results demonstrate that the relative timing between presynaptic stimulation and postsynaptic burst firing determines the direction and the magnitude of NMDAR plasticity.

NMDAR LTP Is Input Specific

The involvement of NMDAR activation in the induction of NMDAR LTP raises the possibility that NMDARs might be potentiated specifically at those synapses stimulated during induction. To test this possibility, we placed two stimulating electrodes more than 100 μm apart from each other. After confirming the independence of the two pathways (see Experimental Procedures), we monitored NMDAR EPSCs in each pathway for 10 min. Once a stable baseline was established, one pathway received sustained synaptic stimulation paired with burst firing while the other pathway was held silent (Figure 6). This produced LTP selectively in the paired pathway (paired pathway: 65% ± 16% change versus unpaired pathway: 2% ± 2% change, n = 4, $p < 0.05$), demonstrating that NMDAR LTP can be input specific.

NMDAR LTP Is Unlikely to Be Associated with a Change in Subunit Composition

It has been shown that bath application of orexin A or DA $D_{1/5}$ receptor agonists produces long-lasting increases in NMDAR EPSCs via changes in the composition of NR2 subunits of NMDARs in DA neurons (Borgland et al., 2006; Schilstrom et al., 2006). An activity-dependent switch in NR2 subunit composition has also been reported at neonatal hippocampal synapses (Bellone and Nicoll, 2007). We therefore tested if burst-dependent LTP of NMDARs in DA neurons is also associated with a change in the subunit composition by comparing the effects of NMDAR subunit specific antagonists on control NMDAR EPSCs versus potentiated EPSCs after successful LTP induction. We used three different NR2 subtype-specific antagonists: Ro 25-6981 (1 μM) and ifenprofil (3 μM), NR2B-containing receptor antagonists, and Zn^{2+} (100 nM), an NR2A-containing receptor antagonist (Fischer et al., 1997; Paoletti et al., 1997; Williams, 1993). None of these antagonists showed differential effects on control versus potentiated NMDAR EPSCs (Figure 7), suggesting that the burst pairing protocol induces NMDAR LTP without a change in the subunit composition of NMDARs.

NMDAR LTP Is Reversible

Synaptic plasticity induced by correlated presynaptic and postsynaptic activity can be reversed by presynaptic stimulation in the absence of postsynaptic activation (Bellone and Nicoll, 2007; Massey and Bashir, 2007). To examine if NMDAR LTP can be reversed (depotentiated) in DA neurons, we repeatedly delivered synaptic stimulation alone (ten times every 20 s) 30 min after inducing LTP of NMDAR EPSCs (30% ± 6% change, n = 4) (Figures 8A and 8B). This depotentiation protocol rapidly depressed previously potentiated NMDAR EPSCs back toward baseline levels in all four neurons tested (baseline: 59 ± 9 pA, LTP: 75 ± 10 pA, postdepotentiation: 57 ± 9 pA). Depotentiation was not associated with a change in either PPR or $1/CV^2$ (0.99 ± 0.10 versus 1.00 ± 0.10 and 19 ± 4 versus 17 ± 4, respectively; $p > 0.5$ for both parameters). It should be noted that the same procedure, i.e., delivery of synaptic stimulation alone, also induced a small but rapid LTD of control EPSCs that had not undergone LTP induction (−8% ± 4% change, n = 6) (Figure 1E).

We next inserted a single AP into the depotentiation protocol at 1 s after the onset of synaptic stimulation, i.e., at the same timing as the burst in the burst pairing protocol (Figures 8C and 8D). Surprisingly, pairing synaptic stimulation with a single AP completely prevented depotentiation in all four neurons tested (baseline: 53 ± 3 pA, LTP: 71 ± 3 pA, post-single AP pairing: 71 ± 3 pA). The same protocol also produced no change in control NMDAR EPSCs (1% ± 8% change, n = 5) (Figure 1E). Thus, synaptic stimulation-single AP pairing had no effect on

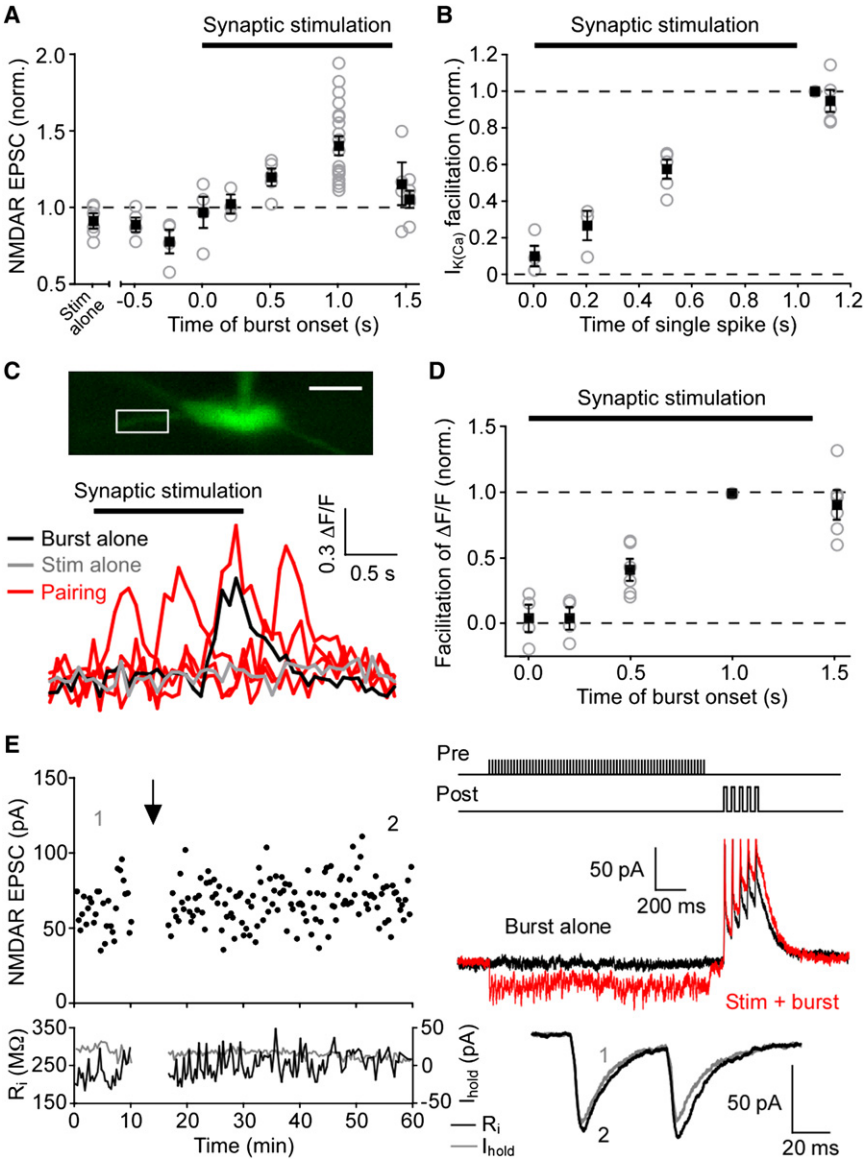

Figure 5. Burst-Timing Dependence of NMDAR Plasticity

(A) Summary graph depicting the burst-timing dependence of NMDAR plasticity. The magnitude of LTP/LTD is plotted versus time of burst onset relative to the onset of 1.4 s synaptic stimulation (black bar) during the induction protocol. Individual experiments are shown as gray open circles; black squares represent mean. Data for the 1 s delay (n = 21) are from control LTP experiments with $I_{K(Ca)}$ facilitation >15% shown in Figure 1B, while the data for synaptic stimulation alone are from Figure 1E.

(B) Summary graph illustrating the timing dependence of $I_{K(Ca)}$ facilitation assessed using 1 s synaptic stimulation. Data are from neurons shown in (A). In order to measure $I_{K(Ca)}$ facilitation, a single AP was evoked at the indicated time relative to 1 s synaptic stimulation. The amount of $I_{K(Ca)}$ facilitation thus obtained was normalized to that measured at 60 ms after the offset of synaptic stimulation in each neuron. Therefore, data for 21 neurons in the control LTP experiments with 1 s delay are all normalized to unity. Gray open circles represent data from individual experiments, while black squares indicate mean.

(C) Example experiment imaging burst-evoked Ca^{2+} signals at various synaptic stimulation-burst timing intervals. Fluorescence changes were measured at the ROI indicated in the confocal fluorescence image of a DA neuron filled with fluo-5F (scale bar: 20 μm). Black and gray traces represent burst alone and synaptic stimulation alone, respectively, whereas red traces represent synaptic stimulation-burst pairing, in which the burst was evoked at onset, 500 ms after onset, 1 s after onset, and 120 ms after offset of 1.4 s synaptic stimulation (black bar).

(D) Summary graph showing the timing dependence of synaptic facilitation of burst-evoked Ca^{2+} signals. Facilitation is plotted versus time of burst onset relative to the onset of 1.4 s synaptic stimulation (black bar). The magnitude of facilitation was normalized to that produced when burst was elicited 1 s after onset of synaptic stimulation in each neuron. Gray open circles represent data from individual experiments, whereas black squares indicate mean.

(E) Example experiment in which the burst was delayed by 120 ms after the offset of synaptic stimulation train, as illustrated at top right. Middle right: Sample traces show the response to postsynaptic burst alone (black) and synaptic stimulation-burst pairing with a 120 ms delay (red). Bottom right: Average EPSCs before (1) and after (2) 120 ms delay pairing taken at the times indicated. Error bars indicate SEM.

NMDAR EPSCs regardless of whether they had been previously potentiated or not. Together, these results demonstrate that NMDAR LTP can be reversed by repetitive synaptic stimulation in the absence of postsynaptic firing activity.

DISCUSSION

Here we have demonstrated that repetitive pairing of sustained synaptic stimulation with burst firing induces LTP of NMDAR EPSCs in midbrain DA neurons. The induction of NMDAR LTP requires (1) synaptic facilitation of burst-evoked Ca^{2+} signals via mGluRs and other PI-coupled receptors generating IP_3, and (2) activation of NMDARs. The burst-timing dependence of LTP induction is consistent with these two requirements in that (1) the burst needs to occur with a certain delay (~0.5–1 s) after the onset of synaptic stimulation, reflecting the time required for synaptic stimulation to cause a rise in IP_3 levels, and (2) the burst also has to take place before or immediately (within tens of milliseconds) after the termination of synaptic stimulation so that NMDARs are activated at the time of the burst. Intriguingly, LTD of NMDAR EPSCs is induced when the burst precedes synaptic stimulation during the induction protocol, although the exact cellular mechanisms underlying bidirectionality of NMDAR plasticity remain to be determined (Harney et al., 2006). The

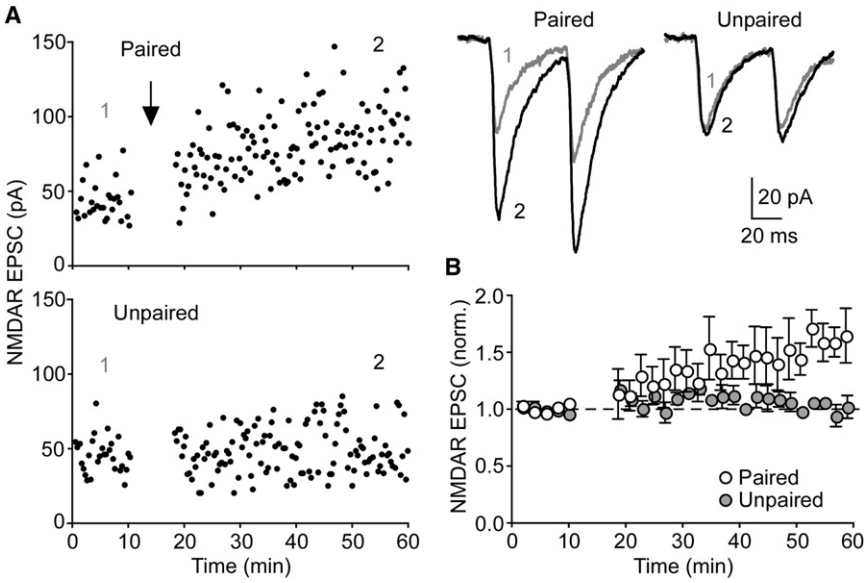

Figure 6. Input Specificity of NMDAR LTP

(A) Time graphs of a representative experiment where two independent pathways were alternately stimulated via two extracellular electrodes. During the induction, only one pathway was stimulated in conjunction with postsynaptic bursting (top, "paired"), while the other pathway was left unstimulated (bottom, "unpaired"). Sample traces show average NMDAR EPSCs taken at the times indicated for the paired (left) and unpaired (right) pathways.

(B) Summary time graph of NMDAR LTP in paired versus unpaired pathways in four neurons. Error bars indicate SEM.

activity-dependent plasticity of NMDARs in this study represents a mechanism for long-term regulation of DA neuron output that might also integrate with other forms of synaptic plasticity dependent on NMDAR activation (Engblom et al., 2008; Nugent et al., 2007; Zweifel et al., 2008).

Induction Mechanisms of NMDAR LTP in DA Neurons

It is well established that Ca^{2+} signals triggered by postsynaptic APs play a critical role in the induction of synaptic plasticity (Linden, 1999; Sjostrom and Nelson, 2002). APs can propagate and trigger Ca^{2+} influx in DA neuron dendrites with high efficiency (Hausser et al., 1995; Wilson and Callaway, 2000). Interestingly, the induction of NMDAR LTP in this study requires burst firing, as pairing synaptic stimulation with a single AP was ineffective at driving plasticity. In addition, burst-induced Ca^{2+} signals need to be amplified by preceding activation of PI-coupled receptors, which recruits CICR via IP_3Rs on intracellular stores, to effectively induce LTP. Why are Ca^{2+} transients resulting from burst-induced Ca^{2+} influx insufficient to drive plasticity by themselves? Perhaps the mechanism is similar to that described for localized Ca^{2+} signaling and LTD of AMPAR EPSCs at parallel fiber synapses on cerebellar Purkinje neurons (Sarkisov and Wang, 2008; Wang et al., 2000). Here, climbing fiber activation and subsequent dendritic Ca^{2+} spike generation do not evoke large enough Ca^{2+} transients in dendritic spines to reach the threshold for plasticity induction unless CICR is triggered by parallel fiber inputs activating mGluRs and producing local IP_3 increases in spines. The main difference between NMDAR LTP in DA neurons and AMPAR LTD in Purkinje neurons is the involvement of NMDAR activation in the induction. At parallel fiber-Purkinje neuron synapses, which lack NMDARs, chemical compartmentalization offered by dendritic spines

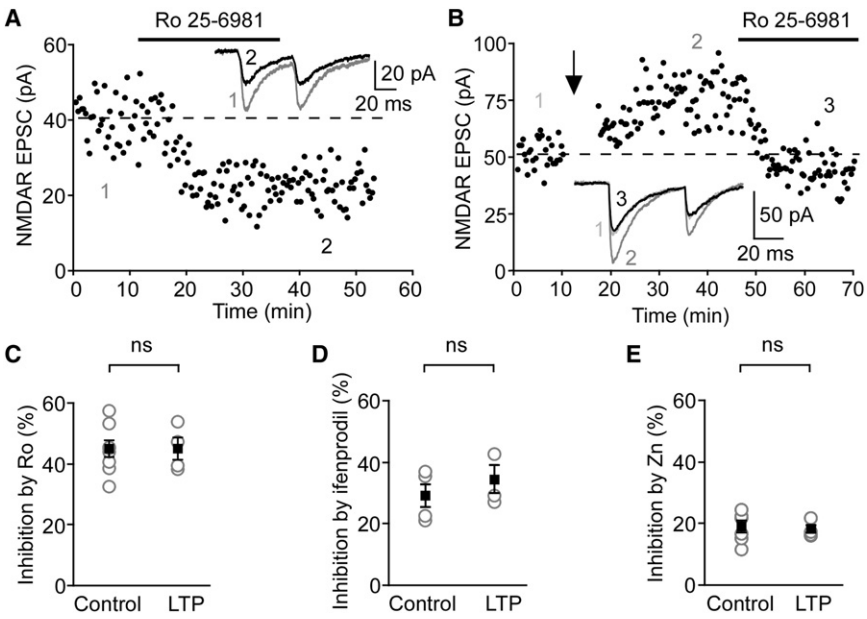

Figure 7. NMDAR LTP Is Unlikely to Be Expressed via a Change in NR2 Subunit Composition

(A) Representative time graph showing the effect of Ro 25-6981 (1 μM) on control NMDAR EPSCs. Ro 25-6981 was perfused during the time indicated by the black bar. Average EPSCs before (1) and after Ro 25-6981 application (2) are shown in inset.

(B) Representative time graph depicting the effect of Ro 25-6981 (1 μM) on NMDAR EPSCs after successful induction of LTP. Burst pairing protocol was delivered at the arrow, while Ro 25-6981 was perfused during the time indicated by the black bar. Inset shows average EPSCs before (1) and after LTP induction (2), together with the average EPSC after Ro 25-6981 application (3).

(C–E) Summary of the effects of Ro 25-6981 (1 μM; C), ifenprodil (3 μM; D), and Zn^{2+} (100 nM; E) on control NMDAR EPSCs (n = 6, n = 4, and n = 6, respectively) and potentiated EPSCs after LTP induction (n = 4, n = 3, and n = 4, respectively). Gray circles indicate data from individual neurons, whereas black squares indicate mean ± SEM.

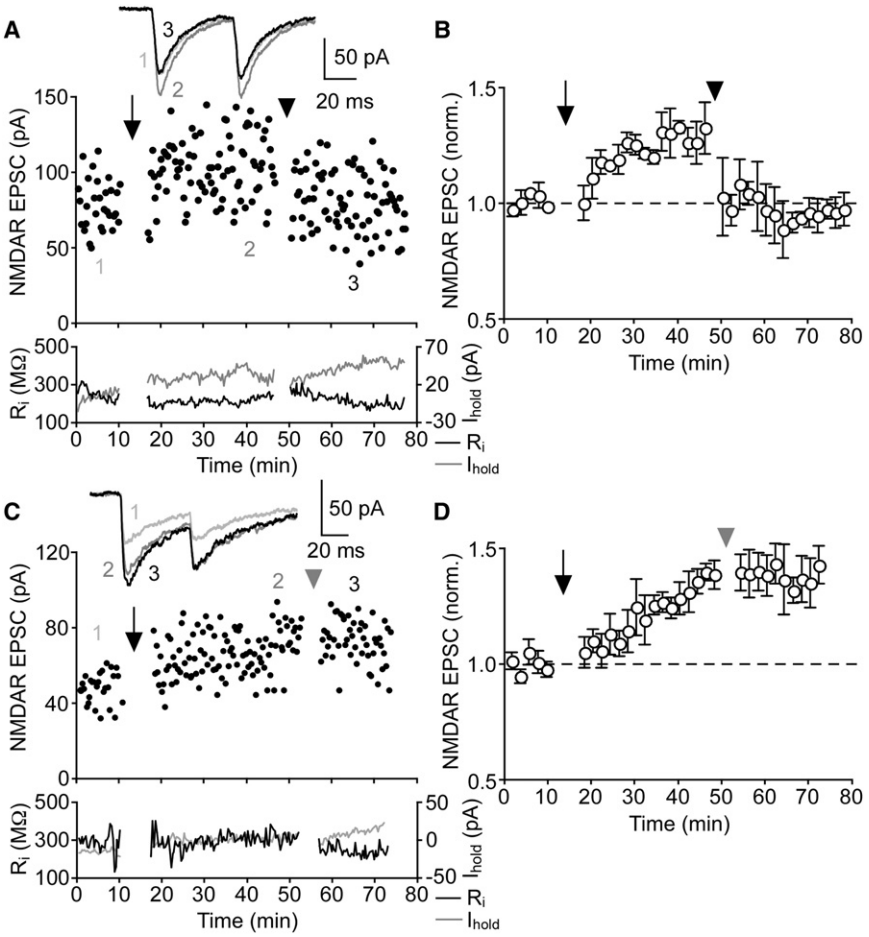

Figure 8. NMDAR LTP Can Be Reversed

(A) Representative experiment showing that repeated synaptic stimulation can depotentiate previously potentiated NMDAR EPSCs. The arrow indicates LTP induction by synaptic stimulation-burst pairing, whereas the arrowhead indicates the delivery of the depotentiation protocol consisting of synaptic stimulation alone. Average NMDAR EPSCs taken at the times indicated are shown in inset for control (1), after LTP (2), and after depotentiation (3).

(B) Summary time graph of depotentiation experiments (n = 4). Burst pairing protocol was delivered at the arrow to induce LTP, while the depotentiation protocol was applied at the arrowhead.

(C) Time course of a representative experiment in which pairing synaptic stimulation with single postsynaptic APs during the depotentiation protocol prevented reversal of previously induced NMDAR LTP. LTP was induced at the arrow, while the synaptic stimulation-single AP pairing protocol was applied at the gray arrowhead. Average NMDAR EPSCs are shown in inset for control (1), after LTP (2), and after single-AP pairing (3).

(D) Summary time graph of experiments attempting depotentiation with single-AP pairing (n = 4). Error bars indicate SEM.

restricts IP_3 and Ca^{2+} signaling to individual spines, thereby mediating synapse specificity of plasticity (Nimchinsky et al., 2002; Wang et al., 2000). However, such compartmentalization of IP_3-dependent Ca^{2+} signaling might not be easily attained at glutamatergic synapses on DA neurons, which are mostly formed on dendritic shafts [(Carr and Sesack, 2000; Charara et al., 1996), but also see (Sarti et al., 2007)]. Indeed, synaptic activation of mGluRs augments burst-induced Ca^{2+} transients throughout individual dendrites in DA neurons (Cui et al., 2007). Therefore, the localized signal underlying the input specificity of NMDAR LTP is presumably provided by NMDARs causing Ca^{2+} influx only at activated synapses, which would be below the spatial resolution of the confocal imaging system used in the present study. In support of this idea, synaptic activation of ionotropic glutamate receptors (i.e, Ca^{2+}-permeable AMPARs) has been shown to produce highly localized (~1 μm) Ca^{2+} transients in aspiny dendrites mediating input-specific Ca^{2+} signaling and plasticity (Goldberg et al., 2003; Soler-Llavina and Sabatini, 2006). The requirement for coactivation of NMDARs and mGluRs, together with the dependence on intracellular Ca^{2+} stores, is in line with recent studies demonstrating input-specific LTP of NMDAR EPSCs at hippocampal mossy fiber synapses (Kwon and Castillo, 2008; Rebola et al., 2008). It should also be noted that Ca^{2+} transients resulting from NMDAR-induced Ca^{2+} influx can be amplified via an mGluR- and IP_3-dependent CICR mechanism at Schaffer collateral synapses on hippocampal CA1 pyramidal neurons (Dudman et al., 2007).

A number of studies have reported LTP of NMDAR-mediated transmission in the hippocampus (Bashir et al., 1991; Bellone and Nicoll, 2007; Harney et al., 2008; Kwon and Castillo, 2008; Rebola et al., 2008), yet none of these studies have addressed the role of postsynaptic APs in LTP induction. A delayed NMDAR LTP has been observed in cortical pyramidal neurons, which is induced by simultaneous presynaptic and postsynaptic burst firing and is dependent on preceding AMPAR LTP (Watt et al., 2004). In the present study, NMDAR LTP required a delay between the onset of presynaptic stimulation and postsynaptic burst firing and was independent of AMPARs. Thus, NMDAR LTP in DA neurons represents a form of Hebbian plasticity of NMDAR-mediated transmission that has not been previously described.

Ample evidence indicates the important role of PKA in regulating different aspects of synaptic plasticity (Nguyen and Woo, 2003). In particular, PKA has been shown to gate the induction of AMPAR LTP by modulating CaMKII and SK2 channels in the hippocampus and amygdala (Blitzer et al., 1998; Faber et al., 2008). Our data show that PKA gates the induction of NMDAR LTP in DA neurons through enhancement of IP_3R function. LTP induction might also be affected by PKA regulation of NMDAR-mediated Ca^{2+} influx (Skeberdis et al., 2006).

Burst-dependent potentiation of NMDARs appears to be expressed postsynaptically by a mechanism distinct from that previously described for metabotropic receptor-induced

potentiation of NMDAR EPSCs in DA neurons (Borgland et al., 2006; Schilstrom et al., 2006; Ungless et al., 2003). For example, activation of orexin-1 receptors induces PKC-dependent translocation of NR2A-containing NMDARs to the synapse (Borgland et al., 2006). PKC-mediated recruitment of NMDARs has also been implicated in NMDAR LTP at hippocampal mossy fiber synapses (Kwon and Castillo, 2008). However, PKC blockade failed to affect NMDAR LTP in our study. Furthermore, the effects of NR2A- and NR2B-specific antagonists on NMDAR EPSCs were not altered after LTP expression. Although we cannot rule out potential changes in NR2C/2D subunits (Harney et al., 2008), these subunits make small contributions to NMDAR EPSCs in DA neurons (Borgland et al., 2006). Therefore, enhanced function of individual NMDAR channels and/or increased synaptic expression of existing NMDARs with no change in the subunit composition likely mediate the expression of LTP (Chen and Roche, 2007).

Burst-Timing Dependence and Reversibility of NMDAR Plasticity in DA Neurons: Potential Relevance to Reward Learning

In behaving animals, DA neurons "learn" to respond to inherently neutral environmental cues with synchronized bursts of activity after repeated cue-reward pairing (Pan et al., 2005; Schultz, 1998). Several modeling studies have addressed the neurobiological substrates underlying the conditioning of DA neuron responses (Brown et al., 1999; Contreras-Vidal and Schultz, 1999; Houk et al., 1995). One of these models postulates that plasticity of synapses onto DA neurons is involved in this learning process (Contreras-Vidal and Schultz, 1999). It has also been shown in awake rats that excitatory responses of pedunculopontine tegmental nucleus neurons to auditory cues, which play an important role in driving DA neuron burst responses to those cues, remain unaltered during cue-reward learning (Pan and Hyland, 2005). Because the pedunculopontine tegmental nucleus gives rise to direct glutamatergic (and cholinergic) inputs to DA neurons (Charara et al., 1996), this raises the possibility that plasticity of glutamatergic synapses onto DA neurons might play a role in the development of conditioned burst responses. Therefore, in light of the prominent role of NMDARs in the generation of DA neuron bursts (Chergui et al., 1994; Morikawa et al., 2003; Overton and Clark, 1997; Tong et al., 1996; Zweifel et al., 2009), the activity-dependent plasticity of NMDARs described in this study might contribute to the acquisition of cue responses. It should be noted that the synaptic stimulation-burst pairing protocol emulates the neural activity evoked during the cue-reward pairing paradigm. Here, sustained synaptic stimulation mimics the working memory-type persistent input activated by the presentation of the cue (Brown et al., 1999; Funahashi et al., 1989), whereas the postsynaptic burst corresponds to that triggered by the reward during conditioning. In this model, potentiated NMDARs at those synapses activated by the cue, accompanied by certain termination mechanism(s) (e.g., SK channel activation), mediate the transient burst response to the cue after conditioning.

Of particular interest is the burst-timing dependence of the induction of NMDAR plasticity, which appears analogous to the timing rule governing cue-reward learning in behaving animals. In the standard and most effective training paradigm, termed delay conditioning, there is a delay of hundreds of milliseconds to several seconds between the onset of the cue and that of the reward, with the two stimuli overlapping in time (Fiorillo et al., 2003; Schwartz et al., 2002). For NMDAR LTP in DA neurons, the requirement of the delay (~0.5–1 s) and the overlap between synaptic stimulation and burst firing during induction most likely reflects the involvement of PI-coupled receptors and NMDARs, respectively. Furthermore, induction of LTD when the burst precedes synaptic stimulation during the burst pairing protocol is congruent with the ineffectiveness of backward conditioning in which the reward is presented before the cue (Schwartz et al., 2002). The timing rule described here is distinct from that for the spike-timing-dependent plasticity reported in a variety of neurons (Dan and Poo, 2004; Sjostrom and Nelson, 2002), including DA neurons (Liu et al., 2005; Luu and Malenka, 2008), in which the plasticity is sensitive to the timing of presynaptic and postsynaptic spikes on a timescale of tens of milliseconds, much shorter than the timescales encountered during behavioral conditioning (Drew and Abbott, 2006).

It is of note that the same induction protocol that caused NMDAR LTP resulted in LTD of AMPAR EPSCs in this study. Because AMPAR LTD did not require postsynaptic bursting, it presumably corresponds to the mGluR-dependent but postsynaptic activity-independent AMPAR LTD mediated by a shift in the AMPAR subunit composition in DA neurons (Mameli et al., 2007). This LTD has been shown to reverse the persistent and global potentiation of AMPARs produced by cocaine administration paired with environmental cues, and thus might act to reset AMPAR-mediated transmission to enable AMPAR plasticity required for future learning (Bellone and Luscher, 2006; Chen et al., 2008; Stuber et al., 2008). Therefore, simultaneous NMDAR LTP and AMPAR LTD might work in concert to promote the learning of new environmental cues in animals previously conditioned with powerful reinforcers such as addictive drugs. However, it is important to point out that the exact, and perhaps differential, roles of NMDAR plasticity versus AMPAR plasticity in vivo remain to be determined.

The neural mechanisms underlying behavioral learning are thought to involve both reversible and irreversible components (Medina et al., 2002; Pan et al., 2008). Our results show that NMDAR LTP can be reversed, or depotentiated, by repeated delivery of synaptic stimulation alone, which is reminiscent of the extinction of learned responses when the conditioning cue is repeatedly presented without the expected reward. It is remarkable that the expression of LTP is maintained when synaptic stimulation is repeatedly paired with a single AP, suggesting that single AP-evoked Ca^{2+} transients, facilitated by IP_3-dependent CICR, can serve to prevent depotentiation. Therefore, a pause in tonic single-spike activity of DA neurons, as observed at the time of the expected reward when the learned cue is presented alone, might be necessary to induce extinction of phasic burst responses to the cue (Pan et al., 2008; Tobler et al., 2003).

EXPERIMENTAL PROCEDURES

Electrophysiology

Horizontal midbrain slices were prepared from male Sprague-Dawley rats (4–7 weeks old). Recordings were made at 34°C–35°C in a chamber perfused

at ~2.5 ml/min with recording solution containing (in mM): 126 NaCl, 2.5 KCl, 1.2 NaH_2PO_4, 1.2 or 0.1 $MgCl_2$, 2.4 $CaCl_2$, 11 glucose, 21.4 $NaHCO_3$, saturated with 95% O_2/5% CO_2 (pH 7.4, ~295 mOsm/kg). The pipette solution contained (in mM): 115 K-gluconate or K-methylsulfate, 20 KCl, 1.5 $MgCl_2$, 10 HEPES, 0.025 EGTA, 2 Mg-ATP, 0.2 Na_2-GTP, and 10 Na_2-phosphocreatine (pH 7.25, 285 mOsm/kg).

Cells were visualized using an upright microscope with IR-DIC optics (Olympus). Whole-cell voltage-clamp recordings were made from electrophysiologically identified DA neurons at a holding potential of −62 mV, corrected for a liquid junction potential of −7 mV. Pipette resistance was 2.0–2.5 MΩ. Pipette capacitance was neutralized but series resistance was left uncompensated. Input resistance (typically ~250 MΩ) and holding current (typically 0 to −100 pA) were monitored continuously; experiments were discarded if they changed by more than 25% or 60 pA, respectively, or if series resistance increased above 16 MΩ. A Multiclamp 700B amplifier (Molecular Devices) was used to record the data, which were filtered at 2–10 kHz, digitized at 4–20 kHz, and collected using AxoGraph X (AxoGraph Scientific).

Synaptic Stimulation and LTP Induction

Synaptic stimuli were applied at 0.05 Hz using bipolar tungsten electrodes (100–120 μm tip separation) and pharmacologically isolated NMDAR EPSCs were monitored.

Immediately before LTP induction, the effect of sustained synaptic stimulation on $I_{K(Ca)}$, evoked by a single unclamped AP, was evaluated in each neuron. A 2 ms depolarizing pulse from −62 mV to −7 mV was used to elicit an unclamped AP. The integral of the outward tail current, i.e., $I_{K(Ca)}$, was calculated between 20 ms and 400–600 ms after the depolarizing pulse. We have shown previously that $I_{K(Ca)}$ thus measured is completely eliminated by TTX and also by apamin, a selective blocker of Ca^{2+}-sensitive SK channels, and hence can be used as a readout of AP-induced Ca^{2+} transients (Cui et al., 2007). The magnitude of $I_{K(Ca)}$ facilitation by synaptic stimulation was calculated by comparing $I_{k(Ca)}$ evoked 60 ms after a 1 s train of 50-Hz synaptic stimulation, after subtracting the trace elicited by synaptic stimulation alone, with $I_{k(Ca)}$ evoked in isolation. A single AP, instead of a burst of APs, was used in evaluating synaptic facilitation of $I_{K(Ca)}$ in order to avoid potential influence on LTP induction.

The LTP induction protocol consisted of sustained synaptic stimulation (70 stimuli at 50 Hz) paired with a postsynaptic burst of five APs at 20 Hz, where the burst was delayed by 1 s from the onset of the synaptic stimulation. Synaptic stimulation was extended 200 ms beyond the end of the burst, i.e., until burst-evoked $I_{k(Ca)}$ mostly decayed, to ensure that synapses were activated while cytosolic Ca^{2+} concentration was elevated. Synaptic stimulation-burst pairing was repeated ten times every 20 s. The same stimulation intensity used for monitoring NMDAR EPSCs was used for synaptic stimulation during induction. The magnitude of LTP was calculated by comparing averaged EPSC amplitudes from 10 min windows (30 traces) immediately before and 30–40 min after LTP induction. These windows were also used to assess PPR and $1/CV^2$.

To test the independence of inputs in the two-pathway experiments (Figure 6), we used cross paired-pulse analysis. We first determined the PPR for each input. We then substituted the opposing input for the second pulse and confirmed the absence of interaction between the two inputs.

Flash Photolysis

Caged IP_3 (100 μM) was loaded into the cytosol through the whole-cell pipette. A 1 ms UV pulse was applied using a xenon arc lamp (Cairn Research) to rapidly release IP_3 and the resulting SK-mediated outward current (I_{IP3}) was measured. The amount of photolysis is known to be proportional to the UV pulse intensity, which is proportional to the capacitance of the capacitor feeding current to the flash lamp. This capacitance was varied (50–4050 μF) to adjust the UV pulse intensity.

Ca^{2+} Imaging

Fluorescence imaging of intracellular Ca^{2+} was performed using fluo-5F (50 μM) loaded into the cytosol via the whole-cell pipette. Images were captured at 15 Hz with a spinning disk confocal imaging system (Olympus). Ca^{2+} signals from selected ROIs were expressed as $\Delta F/F = (F - F_{baseline})/(F_{baseline} - F_{background})$.

Additional methodological details are described in Supplemental Experimental Procedures.

SUPPLEMENTAL DATA

Supplemental Data include five figures, a table, and Supplemental Experimental Procedures and can be found with this article online at http://www.cell.com/neuron/supplemental/S0896-6273(09)00362-6.

ACKNOWLEDGMENTS

We thank Drs. Rishikesh Narayanan and Michael Roberts for comments on the manuscript. We also thank Dr. Michael Mauk for suggesting the single-spike depotentiation experiment. This work was supported by National Institutes of Health Grant DA015687. M.T.H. was supported by a National Science Foundation Graduate Research Fellowship.

Accepted: May 7, 2009
Published: June 24, 2009

REFERENCES

Bashir, Z.I., Alford, S., Davies, S.N., Randall, A.D., and Collingridge, G.L. (1991). Long-term potentiation of NMDA receptor-mediated synaptic transmission in the hippocampus. Nature *349*, 156–158.

Beckstead, M.J., Grandy, D.K., Wickman, K., and Williams, J.T. (2004). Vesicular dopamine release elicits an inhibitory postsynaptic current in midbrain dopamine neurons. Neuron *42*, 939–946.

Bellone, C., and Luscher, C. (2006). Cocaine triggered AMPA receptor redistribution is reversed in vivo by mGluR-dependent long-term depression. Nat. Neurosci. *9*, 636–641.

Bellone, C., and Nicoll, R.A. (2007). Rapid bidirectional switching of synaptic NMDA receptors. Neuron *55*, 779–785.

Blitzer, R.D., Connor, J.H., Brown, G.P., Wong, T., Shenolikar, S., Iyengar, R., and Landau, E.M. (1998). Gating of CaMKII by cAMP-regulated protein phosphatase activity during LTP. Science *280*, 1940–1942.

Blythe, S.N., Atherton, J.F., and Bevan, M.D. (2007). Synaptic activation of dendritic AMPA and NMDA receptors generates transient high-frequency firing in substantia nigra dopamine neurons in vitro. J. Neurophysiol. *97*, 2837–2850.

Bonci, A., and Malenka, R.C. (1999). Properties and plasticity of excitatory synapses on dopaminergic and GABAergic cells in the ventral tegmental area. J. Neurosci. *19*, 3723–3730.

Borgland, S.L., Taha, S.A., Sarti, F., Fields, H.L., and Bonci, A. (2006). Orexin A in the VTA is critical for the induction of synaptic plasticity and behavioral sensitization to cocaine. Neuron *49*, 589–601.

Brown, J., Bullock, D., and Grossberg, S. (1999). How the basal ganglia use parallel excitatory and inhibitory learning pathways to selectively respond to unexpected rewarding cues. J. Neurosci. *19*, 10502–10511.

Carr, D.B., and Sesack, S.R. (2000). Projections from the rat prefrontal cortex to the ventral tegmental area: target specificity in the synaptic associations with mesoaccumbens and mesocortical neurons. J. Neurosci. *20*, 3864–3873.

Charara, A., Smith, Y., and Parent, A. (1996). Glutamatergic inputs from the pedunculopontine nucleus to midbrain dopaminergic neurons in primates: Phaseolus vulgaris-leucoagglutinin anterograde labeling combined with post-embedding glutamate and GABA immunohistochemistry. J. Comp. Neurol. *364*, 254–266.

Chen, B.T., and Rice, M.E. (2001). Novel Ca2+ dependence and time course of somatodendritic dopamine release: substantia nigra versus striatum. J. Neurosci. *21*, 7841–7847.

Chen, B.S., and Roche, K.W. (2007). Regulation of NMDA receptors by phosphorylation. Neuropharmacology *53*, 362–368.

Chen, B.T., Bowers, M.S., Martin, M., Hopf, F.W., Guillory, A.M., Carelli, R.M., Chou, J.K., and Bonci, A. (2008). Cocaine but not natural reward

self-administration nor passive cocaine infusion produces persistent LTP in the VTA. Neuron *59*, 288–297.

Chergui, K., Akaoka, H., Charlety, P.J., Saunier, C.F., Buda, M., and Chouvet, G. (1994). Subthalamic nucleus modulates burst firing of nigral dopamine neurones via NMDA receptors. Neuroreport *5*, 1185–1188.

Contreras-Vidal, J.L., and Schultz, W. (1999). A predictive reinforcement model of dopamine neurons for learning approach behavior. J. Comput. Neurosci. *6*, 191–214.

Cui, G., Bernier, B.E., Harnett, M.T., and Morikawa, H. (2007). Differential regulation of action potential- and metabotropic glutamate receptor-induced Ca2+ signals by inositol 1,4,5-trisphosphate in dopaminergic neurons. J. Neurosci. *27*, 4776–4785.

D'Ardenne, K., McClure, S.M., Nystrom, L.E., and Cohen, J.D. (2008). BOLD responses reflecting dopaminergic signals in the human ventral tegmental area. Science *319*, 1264–1267.

Dan, Y., and Poo, M.M. (2004). Spike timing-dependent plasticity of neural circuits. Neuron *44*, 23–30.

Drew, P.J., and Abbott, L.F. (2006). Extending the effects of spike-timing-dependent plasticity to behavioral timescales. Proc. Natl. Acad. Sci. USA *103*, 8876–8881.

Dudman, J.T., Tsay, D., and Siegelbaum, S.A. (2007). A role for synaptic inputs at distal dendrites: instructive signals for hippocampal long-term plasticity. Neuron *56*, 866–879.

Engblom, D., Bilbao, A., Sanchis-Segura, C., Dahan, L., Perreau-Lenz, S., Balland, B., Parkitna, J.R., Lujan, R., Halbout, B., Mameli, M., et al. (2008). Glutamate receptors on dopamine neurons control the persistence of cocaine seeking. Neuron *59*, 497–508.

Faber, E.S., Delaney, A.J., Power, J.M., Sedlak, P.L., Crane, J.W., and Sah, P. (2008). Modulation of SK channel trafficking by beta adrenoceptors enhances excitatory synaptic transmission and plasticity in the amygdala. J. Neurosci. *28*, 10803–10813.

Fiorillo, C.D., and Williams, J.T. (2000). Cholinergic inhibition of ventral midbrain dopamine neurons. J. Neurosci. *20*, 7855–7860.

Fiorillo, C.D., Tobler, P.N., and Schultz, W. (2003). Discrete coding of reward probability and uncertainty by dopamine neurons. Science *299*, 1898–1902.

Fischer, G., Mutel, V., Trube, G., Malherbe, P., Kew, J.N., Mohacsi, E., Heitz, M.P., and Kemp, J.A. (1997). Ro 25-6981, a highly potent and selective blocker of N-methyl-D-aspartate receptors containing the NR2B subunit. Characterization in vitro. J. Pharmacol. Exp. Ther. *283*, 1285–1292.

Funahashi, S., Bruce, C.J., and Goldman-Rakic, P.S. (1989). Mnemonic coding of visual space in the monkey's dorsolateral prefrontal cortex. J. Neurophysiol. *61*, 331–349.

Goldberg, J.H., Tamas, G., Aronov, D., and Yuste, R. (2003). Calcium microdomains in aspiny dendrites. Neuron *40*, 807–821.

Harney, S.C., Rowan, M., and Anwyl, R. (2006). Long-term depression of NMDA receptor-mediated synaptic transmission is dependent on activation of metabotropic glutamate receptors and is altered to long-term potentiation by low intracellular calcium buffering. J. Neurosci. *26*, 1128–1132.

Harney, S.C., Jane, D.E., and Anwyl, R. (2008). Extrasynaptic NR2D-containing NMDARs are recruited to the synapse during LTP of NMDAR-EPSCs. J. Neurosci. *28*, 11685–11694.

Hausser, M., Stuart, G., Racca, C., and Sakmann, B. (1995). Axonal initiation and active dendritic propagation of action potentials in substantia nigra neurons. Neuron *15*, 637–647.

Houk, J., Adams, J., and Barto, A. (1995). A model of how the basal ganglia generate and use neural signals that predict reinforcement. In Models of Information Processing in the Basal Ganglia, J. Houk, J. Davis, and D. Beiser, eds. (Cambridge, MA: MIT Press), pp. 249–270.

Hyland, B.I., Reynolds, J.N., Hay, J., Perk, C.G., and Miller, R. (2002). Firing modes of midbrain dopamine cells in the freely moving rat. Neuroscience *114*, 475–492.

Jones, S., and Bonci, A. (2005). Synaptic plasticity and drug addiction. Curr. Opin. Pharmacol. *5*, 20–25.

Kauer, J.A., and Malenka, R.C. (2007). Synaptic plasticity and addiction. Nat. Rev. Neurosci. *8*, 844–858.

Kwon, H.B., and Castillo, P.E. (2008). Long-term potentiation selectively expressed by NMDA receptors at hippocampal mossy fiber synapses. Neuron *57*, 108–120.

Lin, M.T., Lujan, R., Watanabe, M., Adelman, J.P., and Maylie, J. (2008). SK2 channel plasticity contributes to LTP at Schaffer collateral-CA1 synapses. Nat. Neurosci. *11*, 170–177.

Linden, D.J. (1999). The return of the spike: postsynaptic action potentials and the induction of LTP and LTD. Neuron *22*, 661–666.

Liu, Q.S., Pu, L., and Poo, M.M. (2005). Repeated cocaine exposure in vivo facilitates LTP induction in midbrain dopamine neurons. Nature *437*, 1027–1031.

Luu, P., and Malenka, R.C. (2008). Spike timing-dependent long-term potentiation in ventral tegmental area dopamine cells requires PKC. J. Neurophysiol. *100*, 533–538.

Malinow, R., and Tsien, R.W. (1990). Presynaptic enhancement shown by whole-cell recordings of long-term potentiation in hippocampal slices. Nature *346*, 177–180.

Mameli, M., Balland, B., Lujan, R., and Luscher, C. (2007). Rapid synthesis and synaptic insertion of GluR2 for mGluR-LTD in the ventral tegmental area. Science *317*, 530–533.

Massey, P.V., and Bashir, Z.I. (2007). Long-term depression: multiple forms and implications for brain function. Trends Neurosci. *30*, 176–184.

Medina, J.F., Repa, J.C., Mauk, M.D., and LeDoux, J.E. (2002). Parallels between cerebellum- and amygdala-dependent conditioning. Nat. Rev. Neurosci. *3*, 122–131.

Mirenowicz, J., and Schultz, W. (1996). Preferential activation of midbrain dopamine neurons by appetitive rather than aversive stimuli. Nature *379*, 449–451.

Montague, P.R., Dayan, P., and Sejnowski, T.J. (1996). A framework for mesencephalic dopamine systems based on predictive Hebbian learning. J. Neurosci. *16*, 1936–1947.

Montague, P.R., Hyman, S.E., and Cohen, J.D. (2004). Computational roles for dopamine in behavioural control. Nature *431*, 760–767.

Morikawa, H., Khodakhah, K., and Williams, J.T. (2003). Two intracellular pathways mediate metabotropic glutamate receptor-induced Ca2+ mobilization in dopamine neurons. J. Neurosci. *23*, 149–157.

Nguyen, P.V., and Woo, N.H. (2003). Regulation of hippocampal synaptic plasticity by cyclic AMP-dependent protein kinases. Prog. Neurobiol. *71*, 401–437.

Nimchinsky, E.A., Sabatini, B.L., and Svoboda, K. (2002). Structure and function of dendritic spines. Annu. Rev. Physiol. *64*, 313–353.

Nugent, F.S., Penick, E.C., and Kauer, J.A. (2007). Opioids block long-term potentiation of inhibitory synapses. Nature *446*, 1086–1090.

Overton, P.G., and Clark, D. (1997). Burst firing in midbrain dopaminergic neurons. Brain Res. Brain Res. Rev. *25*, 312–334.

Paladini, C.A., and Williams, J.T. (2004). Noradrenergic inhibition of midbrain dopamine neurons. J. Neurosci. *24*, 4568–4575.

Pan, W.X., and Hyland, B.I. (2005). Pedunculopontine tegmental nucleus controls conditioned responses of midbrain dopamine neurons in behaving rats. J. Neurosci. *25*, 4725–4732.

Pan, W.X., Schmidt, R., Wickens, J.R., and Hyland, B.I. (2005). Dopamine cells respond to predicted events during classical conditioning: evidence for eligibility traces in the reward-learning network. J. Neurosci. *25*, 6235–6242.

Pan, W.X., Schmidt, R., Wickens, J.R., and Hyland, B.I. (2008). Tripartite mechanism of extinction suggested by dopamine neuron activity and temporal difference model. J. Neurosci. *28*, 9619–9631.

Paoletti, P., Ascher, P., and Neyton, J. (1997). High-affinity zinc inhibition of NMDA NR1-NR2A receptors. J. Neurosci. *17*, 5711–5725.

Rebola, N., Lujan, R., Cunha, R.A., and Mulle, C. (2008). Adenosine A2A receptors are essential for long-term potentiation of NMDA-EPSCs at hippocampal mossy fiber synapses. Neuron *57*, 121–134.

Ren, Y., Barnwell, L.F., Alexander, J.C., Lubin, F.D., Adelman, J.P., Pfaffinger, P.J., Schrader, L.A., and Anderson, A.E. (2006). Regulation of surface localization of the small conductance Ca2+-activated potassium channel, Sk2, through direct phosphorylation by cAMP-dependent protein kinase. J. Biol. Chem. *281*, 11769–11779.

Sarkisov, D.V., and Wang, S.S. (2008). Order-dependent coincidence detection in cerebellar Purkinje neurons at the inositol trisphosphate receptor. J. Neurosci. *28*, 133–142.

Sarti, F., Borgland, S.L., Kharazia, V.N., and Bonci, A. (2007). Acute cocaine exposure alters spine density and long-term potentiation in the ventral tegmental area. Eur. J. Neurosci. *26*, 749–756.

Schilstrom, B., Yaka, R., Argilli, E., Suvarna, N., Schumann, J., Chen, B.T., Carman, M., Singh, V., Mailliard, W.S., Ron, D., and Bonci, A. (2006). Cocaine enhances NMDA receptor-mediated currents in ventral tegmental area cells via dopamine D5 receptor-dependent redistribution of NMDA receptors. J. Neurosci. *26*, 8549–8558.

Schultz, W. (1998). Predictive reward signal of dopamine neurons. J. Neurophysiol. *80*, 1–27.

Schwartz, B., Wasserman, E.A., and Robbins, S.J. (2002). Psychology of learning and behavior, Fifth Edition (New York, NY: W. W. Norton & Company).

Seidler, N.W., Jona, I., Vegh, M., and Martonosi, A. (1989). Cyclopiazonic acid is a specific inhibitor of the Ca2+-ATPase of sarcoplasmic reticulum. J. Biol. Chem. *264*, 17816–17823.

Shin, N., Soh, H., Chang, S., Kim, D.H., and Park, C.S. (2005). Sodium permeability of a cloned small-conductance calcium-activated potassium channel. Biophys. J. *89*, 3111–3119.

Sjostrom, P.J., and Nelson, S.B. (2002). Spike timing, calcium signals and synaptic plasticity. Curr. Opin. Neurobiol. *12*, 305–314.

Skeberdis, V.A., Chevaleyre, V., Lau, C.G., Goldberg, J.H., Pettit, D.L., Suadicani, S.O., Lin, Y., Bennett, M.V., Yuste, R., Castillo, P.E., and Zukin, R.S. (2006). Protein kinase A regulates calcium permeability of NMDA receptors. Nat. Neurosci. *9*, 501–510.

Soler-Llavina, G.J., and Sabatini, B.L. (2006). Synapse-specific plasticity and compartmentalized signaling in cerebellar stellate cells. Nat. Neurosci. *9*, 798–806.

Stuber, G.D., Klanker, M., de Ridder, B., Bowers, M.S., Joosten, R.N., Feenstra, M.G., and Bonci, A. (2008). Reward-predictive cues enhance excitatory synaptic strength onto midbrain dopamine neurons. Science *321*, 1690–1692.

Tang, T.S., Tu, H., Wang, Z., and Bezprozvanny, I. (2003). Modulation of type 1 inositol (1,4,5)-trisphosphate receptor function by protein kinase a and protein phosphatase 1alpha. J. Neurosci. *23*, 403–415.

Taylor, C.W., and Laude, A.J. (2002). IP3 receptors and their regulation by calmodulin and cytosolic Ca2+. Cell Calcium *32*, 321–334.

Tobler, P.N., Dickinson, A., and Schultz, W. (2003). Coding of predicted reward omission by dopamine neurons in a conditioned inhibition paradigm. J. Neurosci. *23*, 10402–10410.

Tong, Z.Y., Overton, P.G., and Clark, D. (1996). Antagonism of NMDA receptors but not AMPA/kainate receptors blocks bursting in dopaminergic neurons induced by electrical stimulation of the prefrontal cortex. J. Neural Transm. *103*, 889–904.

Ungless, M.A., Singh, V., Crowder, T.L., Yaka, R., Ron, D., and Bonci, A. (2003). Corticotropin-releasing factor requires CRF binding protein to potentiate NMDA receptors via CRF receptor 2 in dopamine neurons. Neuron *39*, 401–407.

Wagner, L.E., 2nd, Joseph, S.K., and Yule, D.I. (2008). Regulation of single inositol 1,4,5-trisphosphate receptor channel activity by protein kinase A phosphorylation. J. Physiol. *586*, 3577–3596.

Wang, S.S., Denk, W., and Hausser, M. (2000). Coincidence detection in single dendritic spines mediated by calcium release. Nat. Neurosci. *3*, 1266–1273.

Watt, A.J., Sjostrom, P.J., Hausser, M., Nelson, S.B., and Turrigiano, G.G. (2004). A proportional but slower NMDA potentiation follows AMPA potentiation in LTP. Nat. Neurosci. *7*, 518–524.

Williams, K. (1993). Ifenprodil discriminates subtypes of the N-methyl-D-aspartate receptor: selectivity and mechanisms at recombinant heteromeric receptors. Mol. Pharmacol. *44*, 851–859.

Wilson, C.J., and Callaway, J.C. (2000). Coupled oscillator model of the dopaminergic neuron of the substantia nigra. J. Neurophysiol. *83*, 3084–3100.

Wolfart, J., Neuhoff, H., Franz, O., and Roeper, J. (2001). Differential expression of the small-conductance, calcium-activated potassium channel SK3 is critical for pacemaker control in dopaminergic midbrain neurons. J. Neurosci. *21*, 3443–3456.

Zalutsky, R.A., and Nicoll, R.A. (1990). Comparison of two forms of long-term potentiation in single hippocampal neurons. Science *248*, 1619–1624.

Zweifel, L.S., Argilli, E., Bonci, A., and Palmiter, R.D. (2008). Role of NMDA receptors in dopamine neurons for plasticity and addictive behaviors. Neuron *59*, 486–496.

Zweifel, L.S., Parker, J.G., Lobb, C.J., Rainwater, A., Wall, V.Z., Fadok, J.P., Darvas, M., Kim, M.J., Mizumori, S.J., Paladini, C.A., et al. (2009). Disruption of NMDAR-dependent burst firing by dopamine neurons provides selective assessment of phasic dopamine-dependent behavior. Proc. Natl. Acad. Sci. USA *106*, 7281–7288.